Methyl dynamics for understanding hydrophobic core packing of dynamically different motifs of double-stranded RNA binding domain of protein kinase R

ARTICLE *in* PROTEINS STRUCTURE FUNCTION AND BIOINFORMATICS · FEBRUARY 2005

Impact Factor: 2.63 · DOI: 10.1002/prot.20793 · Source: PubMed

5 AUTHORS, INCLUDING:

Ravi P Barnwal
University of Washington Seattle
20 PUBLICATIONS **161** CITATIONS
SEE PROFILE

Kandala V R Chary
Tata Institute of Fundamental Research
132 PUBLICATIONS **1,255** CITATIONS
SEE PROFILE

Methyl Dynamics for Understanding Hydrophobic Core Packing of Dynamically Different Motifs of Double-Stranded RNA Binding Domain of Protein Kinase R

Ravi P. Barnwal,[1*] Tista R. Chaudhuri,[1] S. Nanduri,[1] J. Qin,[2] and K.V.R. Chary[1]
[1]*Department of Chemical Sciences, Tata Institute of Fundamental Research, Colaba, Mumbai, India*
[2]*Cleveland Clinic Foundation, Cleveland, Ohio*

ABSTRACT **Double-stranded RNA binding domains of human protein kinase R (dsRBD-PKR) regulate distinct cellular functions and the fate of an RNA molecule in the cell. This highly homologous domains present in multiple copies in a number of species, exhibit individual and specific functional specificity. Number of NMR and X-ray crystallographic structural studies reveals that such domains take a common α-β-β-β-α tertiary fold. However, the functional specificities of these domains could be due to the dynamics of the individual amino acid residues, as has been shown earlier in the case of backbone dynamics of ^{15}N-^{1}H of dsRNA binding motifs (dsRBMs) of human protein kinase R (PKR) (Nanduri S, Rahman F, Williams BRG, Qin J. EMBO J 2000;19:5567–5574). To further investigate if the differences in dynamics of the two dsRBMs are restricted to only backbone, or if the side-chain motions are also different to the extent of influencing their packing of the two hydrophobic cores, we have investigated the methyl group dynamics using ^{13}C-methyl relaxation measurements. The results show that the hydrophobic core of dsRBM1 is more tightly packed than dsRBM2, and it seems to undergo less fast scale motions in the subnanosecond regime. Proteins 2006;62:501–508.**

Key words: PKR; dsRBD; protein dynamics; methyl dynamics; hydrophobic core packing; relaxation studies; 2D [^{13}C-^{1}H]-HSQC; T_1; T_2; NOE

INTRODUCTION

The role of internal dynamics in modulating protein structure, dynamics, and stability has been a subject of considerable interest.[2–9] The side-chain dynamics[4,6,10–14] in general and the methyl group dynamics[15–21] in particular, throw light upon the hidden characteristics of the proteins.

The human protein kinase R (PKR) is one of the key antiviral proteins[22] induced by interferons.[23] Interferons are proteins secreted by the cellular defence system during viral infections. In vitro studies have suggested that the PKR is activated by its binding to a double-stranded RNA (dsRNA). On the other hand, in vivo studies have revealed that the enzyme (PKR) is activated by the viral dsRNA or the viral replicative intermediate comprising dsRNA (Fig. 1).

Human PKR is a 551 residue-long protein containing two domains, which are the N-terminal dsRNA-binding regulatory domain and the C-terminal catalytic or kinase domain. Activation of PKR involves phosphorylation of several serine and threonine residues, which are present in the polypeptide segment linking the two domains. Mutations of these residues (Thr^{258}, Thr^{255}, and Ser^{242}) attenuate kinase activity,[24] indicating an autoregulatory function for this region. Different forms of PKR show different functional roles.[25]

The N-terminal regulatory domain has two dsRNA binding motifs (the N- and the C-terminal motifs, abbreviated as dsRBM1 and dsRBM2, respectively), each about 70 residues long, which are connected by a 20–22 residue-long flexible polypeptide segment. Structural studies by NMR and X-ray crystallography reveal that both motifs have a common tertiary fold, such as α-β-β-β-α. The 3D structure of dsRBD-PKR (PDB ID: 1QU6) indeed shows such a tertiary fold for both motifs. Interestingly, these domains exhibit specific functions, which are different from one another. Such differential functional specificities of these domains could be due to variations in the internal dynamics of the individual amino acid residues, as has been shown earlier in the case of backbone dynamics of dsRNA binding motifs of human PKR.[1]

In this backdrop, we attempted to investigate whether the observed differences in dynamics of these two domains are restricted to only backbone or are extended to side chains, which in turn, could influence their packing in the two individual hydrophobic cores of the protein. We de-

The Supplementary Material referred to in this article can be found online at http://www.interscience.wiley.com/jpages/0887-3585/supmatt/.

Grant sponsor: the National Facility for High Field NMR, supported by Department of Sciences and Technology (DST); Grant sponsor: Department of Biotechnology (DBT); Grant sponsor: Council of Scientific and Industrial Research (CSIR); Grant sponsor: Tata Institute of Fundamental Research (TIFR), Mumbai.

*Correspondence to: Ravi P. Barnwal, Department of Chemical Sciences, Tata Institute of Fundamental Research, Homi Bhabha Road, Colaba, Mumbai-400005, India. E-mail: barnwal@tifr.res.in

Received 1 May 2005; Revised 17 August 2005; Accepted 30 August 2005

Published online 18 November 2005 in Wiley InterScience (www.interscience.wiley.com). DOI: 10.1002/prot.20793

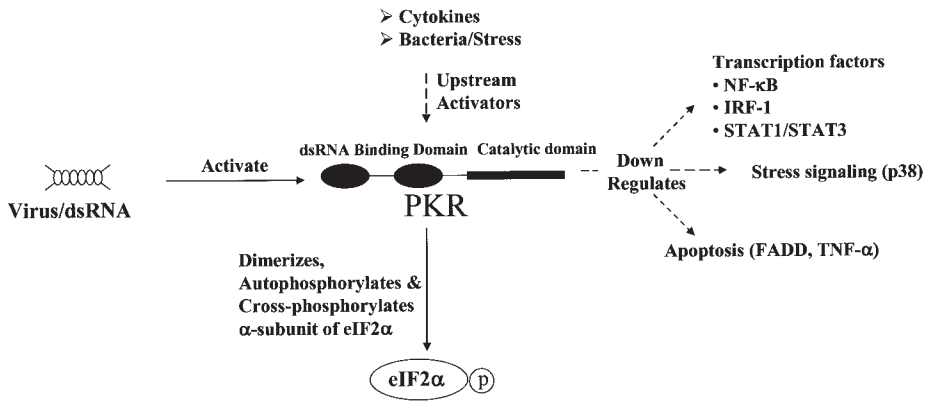

Fig. 1. Role of PKR in different signaling pathways. Binding of viral RNA activates PKR. Cytokines or the stress signaling protein kinases are the upstream PKR activators. The downstream regulators are phosphorylated by the activated PKR.

scribe attempts to understand the dynamics of various methyl groups present in dsRBD-PKR using ^{13}C-methyl relaxation experiments.

RESULTS AND DISCUSSION

Theory of Methyl Dynamics

Methyl dynamics of dsRBD-PKR has been studied using ^{13}C spin-lattice relaxation times (T_1), ^{13}C spin-spin relaxation times (T_2), and steady-state ^{13}C-^{1}H nuclear Overhauser effects (NOEs) data obtained from 2D [^{13}C-^{1}H] NMR spectroscopy. The relaxation data have been analyzed using the model-free approach.[26a,26b] Models of spectral density functions were selected for each residue using the procedure described by Mandel et al.,[27] for both isotropic and axially symmetric diffusion tensors. They are essentially S^2-τ_m, S^2-τ_m-τ_e, S^2-τ_m-R_{ex}, S^2-τ_m-τ_e-R_{ex}, and S_f^2-τ_m-$\tau_{e/s}$-S_s^2, where τ_m is the global correlation time of the molecule, S^2 represents the ^{13}C-^{1}H bond order parameter, S_f^2 and S_s^2 are the order parameters for fast and slow time scale internal motion of the C—H bond, respectively, τ_e or τ_s is the effective correlation time for internal motions and R_{ex} refers to the conformational exchange rate constant. In the first stage, the best model for individual residues was selected by fitting the experimental data to different models separately. In such a selection, the criterion has been a model that required a minimum number of parameters to fit the experimental data. After selection of the best model, τ_m was optimized along with other model parameters using the grid search method.[27] The individual optimizations involved the minimization of χ^2 function using the program Modelfree (4.01).[27] To ascertain whether the relaxation data fitted using R_{ex} terms arise from rotational diffusion anisotropy or conformational exchange, a model incorporating anisotropic diffusion was tested for dsRBD-PKR in a fashion similar to the one described by Tjandra et al.[28]

^{13}C-Methyl Relaxation Analysis

The dsRBD-PKR has 14 Ala, 8 Ile, 16 Leu, 5 Met, 9 Thr, and 7 Val, which possess CH_3 groups. The 3-^{13}C labeled sodium pyruvate used as the amino acid precursor is expected to label only Ala$^{\beta}$, Ile$^{\gamma}$, Leu$^{\delta1,\delta2}$, and Val$^{\gamma1,\gamma2}$. The dsRBM1 contains 5 Ala, 3 Ile, 5 Leu, and 4 Val (26 methyl groups in total), the dsRBM2 has 6 Ala, 5 Ile, 6 Leu, and 2 Val (27 methyl groups), the interdomain linker has 1 Ala, 4 Leu and 1 Val (11 methyl groups), and the polypeptide stretch at the N-terminal end (which is not treated as part of dsRBM1) contains 2 Ala and 1 Leu (4 methyl groups) (Fig. 2). Thus, one would expect 68 crosspeaks in the 2D [^{13}C-^{1}H]-HSQC spectrum recorded with ^{13}C-(methyl)-labeled dsRBD-PKR (Fig. 3). However, we could account for only 42 nonoverlapping peaks, which are amenable for detailed relaxation data analysis. The rest of the methyl crosspeaks suffer from spectral overlaps. Out of these 42 methyl probes, 19 belong to dsRBM1, 10 each to dsRBM2 and to the linker region, and 3 to the polypeptide stretch at the N-terminal end.

^{13}C-T_1, ^{13}C-T_2, and steady-state ^{13}C-^{1}H NOEs were measured following the procedure described in Materials and Methods (Fig. 4). The average T_1, T_2, NOE, and S^2 values of all the methyl group containing residues present in dsRBM1 and dsRBM2 are given in Table 1. Further, the average S^2 values for the individual secondary structural elements are also presented in Table I, separately for dsRBM1 and dsRBM2. As seen from the table, the average T_1 values for both the motifs are almost similar (0.50 and 0.49). However, large discrepancies are seen for the two motifs in the average values of T_2, NOE, and S^2. The motional parameters for the two motifs are on an average taken over 19 and 10 measured values, for dsRBM1 and dsRBM2, respectively. However, for meaningful comparison we have randomly deleted 9 out of 19 measured values of T_1, T_2, NOE, and calculated values of S^2 for dsRBM1, and took an average over the remaining 10 for five times. It is interesting that either way, the average T_1 values remain same for both motifs in the protein and discrepancies noticed earlier in the average values of T_2, NOE, and S^2 between the two motifs remain same. The average T_2 for dsRBM1 is 0.09, while it is 0.14 for dsRBM2. On the other hand, the average NOE value is 1.31 for dsRBM1, while it is 1.14 for dsRBM2. As the smaller T_2 values and higher NOE are indicative of rigid

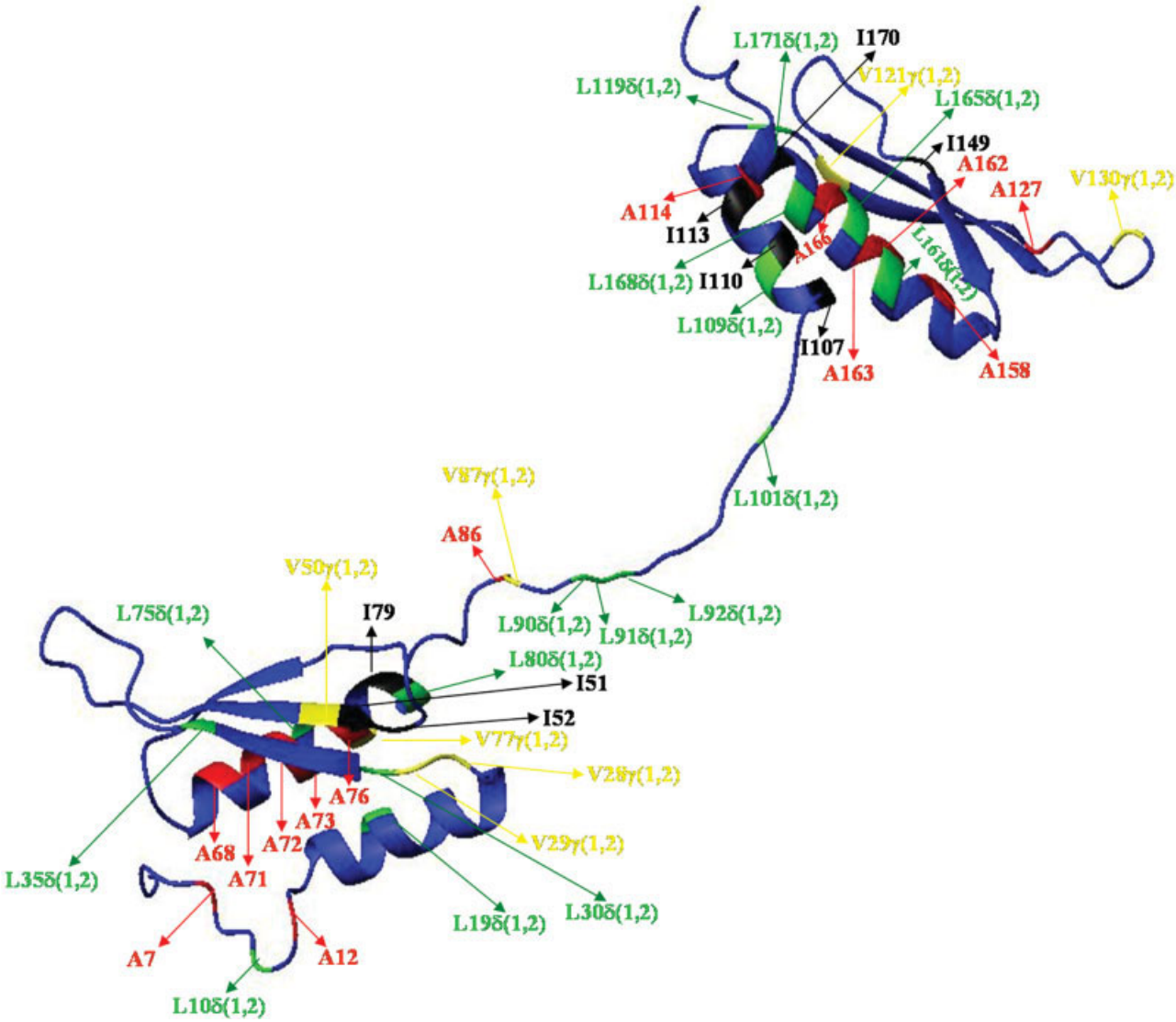

Fig. 2. The annotated picture for all methyl containing amino acid residues in dsRBD-PKR using Molmol[37] (http://hugin.ethz.ch/wuthrich/software/molmol/index.html); alanines are shown in red, isoleucines in black, leucines in green, and valines in yellow. Methionines and threonines, which also contain CH_3 groups, are not annotated.

conformation, one can conclude that dsRBM1 is relatively more rigid compared to dsRBM2. This is also supported by the higher average value of S^2 for dsRBM1 compared to dsRBM2. Further, as seen in Figure 4, the methyl groups belonging to various secondary structural elements in the protein show smaller T_2 (<0.10 s) and higher NOE value (>1.2). The methyl groups in the interdomain linker region (85–106) exhibit higher T_2 values (~0.20 s) and smaller NOEs [Fig. 4(B, C)]. This is similar to the observations made earlier based on the ^{15}N relaxation data.[1] This type of higher flexibility seen in the linker region compared to the two motifs suggests that the two motifs reorient independently as in the case of calmodulin.[29] These observations also support earlier conclusions that interdomain linker region may restrict the reorientation of both dsRBMs to some extent, resulting in some anisotropic motion.[30] In the light of these observations, both isotropic (1.06)[31] and anisotropic (axially symmetric) ($D_{\parallel}/D_{\perp} = 1.20$)[28,32] models were considered in the ^{13}C-methyl relaxation data analysis. The results obtained by considering both the models turned out to be comparable showing that the small anisotropy inflicted by the interdomain linker plays a negligible role on the dynamics of individual methyl groups belonging to both dsRBM1 and dsRBM2. We have used the results obtained using the anisotropic models.

The ^{13}C relaxation data were fitted to model-free spectral density functions using five different sets of motional parameters: (1) S^2; (2) S^2-τ_e; (3) S^2-R_{ex}; (4) S^2-τ_e-R_{ex}; and (5) $S_f{}^2$-τ_s-S_s^2. The overall correlation time for dsRBD-PKR was assumed as 9.53 ± 0.03 ns.[1,33] This is based on ^{15}N relaxation study on dsRBM reported earlier,[1] which has been estimated from the ^{15}N T_1/T_2

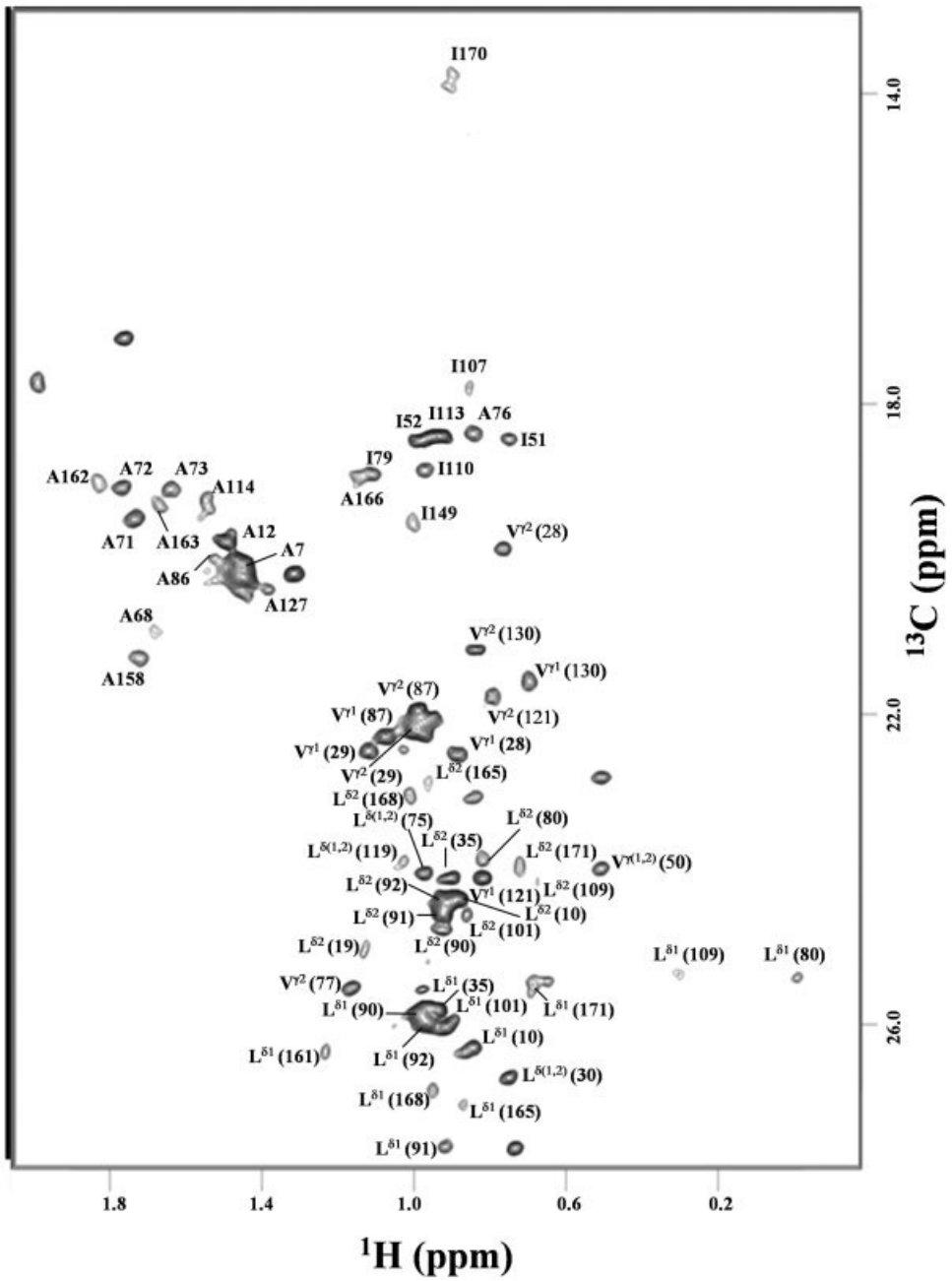

Fig. 3. Selected region of 2D [^{13}C-^{1}H] HSQC spectrum of 0.6 mM uniformly ^{13}C-(methyl) labeled dsRBD-PKR at 25°C, pH 6.5, in 92% H_2O and 8% $^{2}H_2O$ with 20 mM sodium phosphate buffer and 1 mM DTT. The spectrum was acquired with 1024 complex points along t_2 and 256 complex points along t_1. The assignments are labeled with single-letter code of amino acid residues followed by the sequence number and the stereospecificity of the methyl group. The assignment is identical to the published data (BMRB ID: 4110).

ratios of all the residues whose NOE values were at least 0.6 (to make sure that the residues are rigid and have no internal motions). The number of methyl groups that satisfy different models mentioned above are listed in Table II. There is no single methyl group, which satisfies all the models. The ^{13}C relaxation parameters calculated from the respective spectral density functions are found to be comparable with experimental values and thus aided in optimizing model-free parameters. The internal motions on the picosecond time scale were identified from the internal correlation time, τ_e (τ_s) both in Model 2 and Model 5. The extended model-free approach models show that the residues have significant amplitude for internal motions on both nanosecond and picosecond time scale. In such model-free analyses, no R_{ex} values are found. This indicates that there is no microsecond–millisecond motion, which is observed in the event of any conformational exchange. The model-

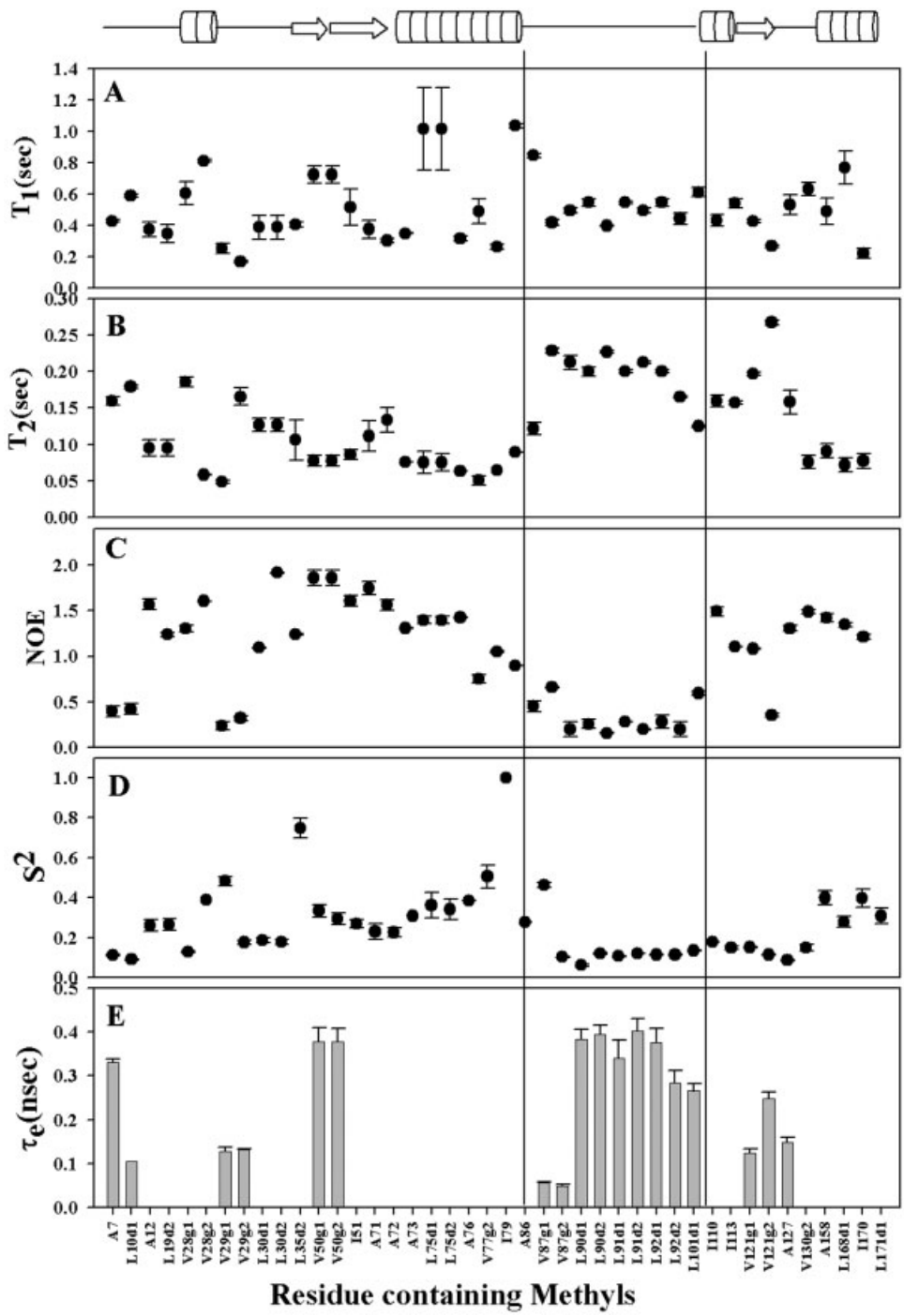

Fig. 4. Methyl-^{13}C-relaxation parameters of dsRBD-PKR. (**A**) T_1, (**B**) T_2, and (**C**) [^{13}C-^{1}H]-NOEs data. Model-free parameters (**D**) S2, and (**E**) τ_e were derived from the anisotropic model.[32,33] The secondary structure elements of the protein are shown on top of the figure. Arrows (⇒) denote β-sheets and cylinders (▭) denote α-helices. The vertical lines highlight the interdomain linker region.

free output results are shown in Figure 4(D, E), which provides information on individual order parameters (S^2) for the methyl ^{13}C-^{1}H vectors and corresponding fast internal motions (τ_e or τ_s). The order parameter S^2 for individual ^{13}C-methyl groups represent the degree of rigidity in side chain that show restricted motions on the picosecond–nanosecond time scale.

Hydrophobic Core-Packing and Internal Motions in dsRBD

As reported earlier,[1] the average S^2 values of individual α-helices and β-sheets (derived from backbone ^{15}N- relaxation study) for the dsRBM1 are smaller than those in dsRBM2, with an exception for β1 in dsRBM1 versus β4 in

TABLE I. Comparison of Methyl Dynamics Parameter for dsRBM1 and dsRBM2 in dsRBD-PKR

	dsRBM1 (15–84)[a]	dsRBM2 (107–174)
Motional parameters for all the ^{13}C-methyl containing residues		
Average T_1(s)	0.50(0.50)	0.49
Average T_2(s)	0.09(0.09)	0.14
Average NOEs	1.31(1.30)	1.14
Average S^2	0.36(0.36)	0.22
Average S^2 of α-helix, β-sheet, and loop		
dsRBM1 dsRBM2		
α1 (15–26) vs. α3 (107–117)	0.26	0.16
loop1 (27–30) vs. loop6 (118–120)	0.26	—
β1 (31–38) vs. β4 (121–128)	0.74	0.12
loop2 (39–45) vs. loop7 (129–135)	—	0.15
β2 (46–54) vs. β5 (136–144)	0.30	—
loop3 (55–59) vs. loop8 (145–149)	—	—
β3 (60–63) vs. β6 (150–153)	—	—
loop4 (64–65) vs. loop9 (154–155)	—	—
α2 (66–84) vs. α4 (156–174)	0.42	0.35
Interdomain linker region (85–106)		0.16

[a]The values in the parentheses are average values calculated by considering only 10 out of the 19 measured values of dsRBM1 for direct comparison with that of dsRBM2.

TABLE II.

Parameter optimized	Number of methyl-containing residues
S^2	24
S^2 and τ_e	15
S^2 and R_{ex}	None
S^2, τ_e and R_{ex}	None
S^2, S_f^2 and τ_e	3

dsRBM2. The observed differences are small indicating that the respective elements have slightly different rigidity. This has also been noticed in loops and turns. In contrast, our study shows that the methyl containing residues in various α-helices, β-sheets, and loops belonging to dsRBM1 in general, have substantially higher values of S^2 compared to the residues belonging to dsRBM2 (Table I). This indicates that the methyl residues of dsRBM1 are much more core-packed than in the dsRBM2. For example, the methyl containing residues in the β1-sheet belonging to dsRBM1 have an average S^2 value of 0.74 compared to the average S^2 value (0.12) for residues in the β4-sheet. However, such a comparison could not be made for all the corresponding secondary structure elements because of insufficient data. For example, loop 2 belonging to dsRBM1, which is involved in dsRNA binding, has no methyl containing residue. The corresponding loop (loop7) in dsRBM2 has two methyl-containing residues. The ^{13}C-relaxation data from these methyl groups reveal that their average S^2 value is small (0.15). Thus, although we can not make any direct comparison between the flexibility of loops 2 and 7, we can conclude that loop 7 is definitely very flexible. This partially supports earlier conclusion that loop 7 is involved in dsRNA-binding.[1]

Figure 4(E) shows polypeptide stretches in dsRBD-PKR with fast internal motions in the picosecond–nanosecond time scale. These segments include residues belonging to secondary structures, β2 (46–54) and β4 (121–128), and the interdomain linker region (85–106) as well as the loop 1 (27–30). The relaxation data for these segments could be fitted with both the Models 2 and 5.

From Figure 4, it can be concluded that the terminal regions are less core-packed, which is also evident from relatively higher values of T_2 and very less NOEs. Methyl groups belonging to the central interdomain linker region (85–106) also show smaller average S^2 value (0.16) and fast internal motions in the picosecond–nanosecond time scale, which indicates higher flexibility of this region.[1]

In conclusion, the study reveals that the hydrophobic core of dsRBM1 is more tightly packed than dsRBM2, and it seems to undergo lesser fast scale motions in the subnanosecond regime.

MATERIALS AND METHODS

Sample Preparation

The dsRBD-PKR was overexpressed and purified following the protocol described earlier.[17b] To uniformly label all the methyl groups present in dsRBD-PKR, the corresponding amino acid precursor, 3-^{13}C labeled sodium pyruvate (99% Isotec) was added to the bacterial culture. To economize the protein production, the amount of the 3-^{13}C labeled sodium pyruvate added was 2.5g/L. This was compensated with 1.5 times higher growth time. The protein thus prepared was concentrated to 250 μL for NMR studies. The protein sample was finally made into a phosphate buffer containing 20 mM NaH_2PO_4, pH 6.5, 150 mM NaCl, 1 mM EDTA, 1 mM DTT in an admixture of 92% H_2O and 8% ^2H_2O. The protein concentration (0.6 mM) was estimated using absorbance at 280 nm (ϵ_{280} = 9200 M^{-1} cm^{-1}) on a SP 75 UV/VIS spectrophotometer (SANYO Biomedical Europe BV). NMR experiments were performed at 25°C. The 2D [^{13}C-^{1}H] HSQC spectrum recorded with the protein sample thus prepared showed the expected signature of crosspeaks arising from all the methyl group containing residues (Fig. 3).

NMR Experiments and Data Analysis

NMR experiments were carried out on a Varian INOVA 600 MHz NMR spectrometer equipped with a pulsed field gradient unit and a triple resonance probe with actively shielded Z-gradients, operating at a ^{1}H frequency of 600.051 MHz.

Experiments with uniformly ^{13}C-methyl labeled dsRBD-PKR sample, essentially included 2D [^{13}C-^{1}H]-HSQC[34,35] and its other versions for the collection of ^{13}C relaxation data (T_1, T_2, and NOE).[16,17a] The crosscorrelation effects

among the three C—H dipolar vectors during the relaxation were suppressed to a large extent by sandwiching 120° ^{1}H pulses between the relaxation pulses. This partially decouples protons with respect to each other. Further, we considered only the beginning of the relaxation data in the analysis of ^{13}C-methyl relaxation study to avoid any residual crosscorrelation effects. This is considered as a fairly good approximation as the double exponential relaxation due to crosscorrelation is described as:[36]

$$I(t) = 1/2\{I(0)[\exp(-(R + R_{cc})t) + \exp(-(R - R_{cc})t)]\}$$

which for $t << (R+R_{cc}), (R-R_{cc})$ becomes

$$I(t) = \frac{1}{2}\{I(0)[1 - (R + R_{cc})t + 1 - (R - R_{cc})t]\}$$

$$= I(0)[1 - R(t)]$$

where R and R_{cc} are the relaxation rates due to longitudinal/transverse relaxation and crosscorrelation, respectively. Thus, we could overcome the crosscorrelation effects and each relaxation data could be fitted to a single exponential. As an illustrative example, some of the fitted data is shown in the supplementary figure (Fig. S1).

In T_1 measurements, the experiments were carried out with delay times of 10, 50,* 110, 170,* 260, 350*, and 490 ms. For T_2 measurements, the experiments were performed with delay times of 5, 10, 20,* 35, 45, 90*, and 130 ms. The experiments with the asterisk (*) were run twice to check the reproducibility of relaxation measurements. The NOE measurements were made both with and without presaturation. The one with a presaturation period of 3.5 s was acquired with a recycle delay of 3.5 s, and other one without presaturation was run with a recycle delay of 7 s. NOEs were measured by taking the ratios of individual peaks in the spectra recorded with and without presaturation ($I_{\text{withpresat}}/I_{\text{withoutpresat}}$). 2D [^{13}C-^{1}H]-HSQC spectra were recorded before and after the collection of the entire relaxation data to check the stability of the protein. No changes were noticed during the entire course of relaxation data measurements, which took around 96 h in total. The relaxation data were processed on a PC using the Felix 97 software (Molecular Simulations Inc.). The spectra were typically apodized using a 60°-shifted sine square bell window function before zero-filling in both the dimensions, followed by 2D Fourier transformation. R_1, R_2, and steady-state NOE spectra were processed to achieve maximum peak heights. Intensities (or peak heights; in arbitrary units) for various ^{1}H-^{13}C crosspeaks in these spectra were measured using the Felix software. The standard deviations are <5% for all the relaxation data. Model-free parameters were fitted according to the protocols described earlier.[32] ^{1}H chemical shifts were calibrated relative to 2,2-dimethyl-2-silapentane-5-sulfonate (DSS). ^{13}C chemical shifts were calibrated indirectly relative to DSS. The assignment of various nonoverlapping methyl ^{13}C-^{1}H crosspeaks was carried out based on the previous knowledge of both ^{1}H and ^{13}C resonance assignments (BMRB ID: 4110). No observable difference was noticed in the chemical shifts for both ^{1}H and ^{13}C.

ACKNOWLEDGMENTS

Ravi P. Barnwal is the recipient of TIFR Endowment Fellowship. We gratefully acknowledge A.G. Palmer for the extended model-free software, Lewis E. Kay for one of the pulse sequences used in this study, and Prof. G. Govil for his critical comments.

REFERENCES

1. Nanduri S, Rahman F, Williams BRG, Qin J. A dynamically tuned double-stranded RNA binding mechanism for the activation of antiviral kinase PKR. EMBO J 2000;19:5567–5574.
2. Debrunner PG, Frauenfelder H. Dynamics of proteins. Annu Rev Phys Chem 1982;33:283–299.
3. Englander SW, Kallenbach NR. Hydrogen exchange and structural dynamics of proteins and nucleic acids. Q Rev Biophys 1983;16:521–655.
4. Frauenfelder H, Sligar SG, Wolynes PG. The energy landscapes and motions of proteins. Science 1991;254:1598–1603.
5. Ishima R, Torchia DA. Protein dynamics from NMR. Nat Struct Biol 2000;7:740–743.
6. Karplus M, McCammon JA. Dynamics of proteins: elements and function. Annu Rev Biochem 1983;52:263–300.
7. Kay LE. Protein dynamics from NMR. Nat Struct Biol NMR Suppl 1998;5:513–517.
8. Palmer AG. Probing molecular motion by NMR. Curr Opin Struct Biol 1997;7:732–737.
9. Williams RJP. NMR studies of mobility within protein structure. Eur J Biochem 1989;183:479–497.
10. Henry GD, Weiner JH, Sykes BD. Backbone dynamics of a model membrane protein: carbon-13 NMR spectroscopy of alanine methyl groups in detergent-solubilized M13 coat protein. Biochemistry 1986;25:590–598.
11. LeMaster DM, Kushlan DM. Dynamical mapping of *E. coli* thioredoxin via ^{13}C NMR relaxation analysis. J Am Chem Soc 1996;118:9255–9264.
12. (a) Li Z, Raychaudhuri S, Wand AJ. Insights into the local residual entropy of proteins provided by NMR relaxation. Protein Sci 1996;5:2647–2650; (b) Wand AJ, Urbauer JL, McEvoy RP, Bieber RJ. Internal dynamics of human ubiquitin revealed by ^{13}C-relaxation studies of randomly fractionally labeled protein. Biochemistry 1996;35:6116–6125.
13. (a) Nardo AAD, Larson SM, Davidson AR. The relationship between conservation, thermodynamics stability, and function of the SH_3 domain hydrophobic core. J Mol Biol 2003;333:641–655; (b) Northey JGB, Nardo AAD, Davidson AR. Hydrophobic core packing in the SH_3 domain folding transition state. Nat Struct Biol 2002;9:126–130.
14. Yamazaki T, Muhandiram R, Kay LE. NMR Experiments for the measurement of carbon relaxation properties in highly enriched, uniformly ^{13}C, ^{15}N-labeled proteins: application to ^{13}C.alpha. carbons. J Am Chem Soc 1995;116:8266–8278.
15. Liu W, Flynn PF, Fuentes EJ, Kranz JK, McCormick M, Wand AJ. Main chain and side chain dynamics of oxidized flavodoxin from *Cyanobacterium anabaena*. Biochemistry 2001;40:14744–14753.
16. Nicholson LK, Kay LE, Baldisseri DM, Arango J, Young PE, Bax A, Torchia DA. Dynamics of methyl groups in proteins as studied by proton-detected ^{13}C NMR spectroscopy. Application to the leucine residues of staphylococcal nuclease. Biochemistry 1992;31:5253–5263.
17. (a) Lee AL, Flynn PF, Wand AJ. Comparison of ^{2}H and ^{13}C NMR relaxation techniques for the study of protein methyl group dynamics in solution. J Am Chem Soc 1999;121:2891–2902; (b) Lee AL, Urbauer JL, Wand AJ. Improved labeling strategy for 13C relaxation measurements of methyl groups in proteins. J Biomol NMR 1997;9:437–440.
18. Hajduk PJ, Augeri DJ, Mack J, Mendoza Re, Yang J, Betz SF, Fesik SW. NMR-based screening of proteins containing ^{13}C-labeled methyl groups. J Am Chem Soc 2000;122:7898–7904.
19. Walsh STR, Lee AL, DeGrado WF, Wand AJ. Dynamics of a de novo designed three-helix bundle protein studied by ^{15}N, ^{13}C, and ^{2}H NMR relaxation methods. Biochemistry 2001;40:9560–9569.
20. Skrynnikov NR, Mulder FAA, Hon B, Dahlquist FW, Kay LE. Probing Slow time scale dynamics at methyl-containing side chains in proteins by relaxation dispersion NMR measurements:

application to methionine residues in a cavity mutant of T4 lysozyme. J Am Chem Soc 2001;123:4556–4566.
21. Mulder FAA, Hon B, Mittermaier A, Dahlquist FW, Kay LE. Slow Internal dynamics in proteins: application of nmr relaxation dispersion spectroscopy to methyl groups in a cavity mutant of T4 lysozyme. J Am Chem Soc 2002;124:1443–1451.
22. Samuel CE. Antiviral actions of interferons. Clin Microbiol Rev 2001;14:778–809.
23. Meurs E, Chong K, Galabru J, Thomas NS, Kerr IM, Williams BRG, Hovanessian AG. Molecular cloning and characterization of the human double-stranded RNA-activated protein kinase induced by interferon. Cell 1990;62:379–390.
24. Taylor DR, Lee SB, Romano PR, Marshak DR, Himmebusch AG, Esteban M, Mathews MB. Autophosphorylation sites participate in the activation of the double-stranded-RNA-activated protein kinase PKR. Mol Cell Biol 1996;16:6295–6302.
25. Jeffrey IW, Kadereit S, Meurs EF, Metzger T, Bachmann M, Schwemmle M, Hovanessian AG, Clemens MJ. Nuclear localization of the interferon-inducible protein kinase PKR in human cells and transfected mouse cells. Exp Cell Res 1995;218:17–27.
26. (a) Lipari G, Szabo A. Model-free approach to the interpretation of nuclear magnetic resonance relaxation in macromolecules. 1. Theory and range of validity. J Am Chem Soc 1982;104:4546–4559; (b) Lipari G, Szabo A. Model-free approach to the interpretation of nuclear magnetic resonance relaxation in macromolecules. 2. Analysis of experimental results. J Am Chem Soc 1982;104:4559–4570.
27. Mandel AM, Akke M, Palmer AG. Backbone dynamics of *Escherichia coli* ribonuclease HI: correlations with structure and function in an active enzyme. J Mol Biol 1995;246:144–163.
28. Tjandra N, Feller SE, Pastor RW, Bax A. Rotational diffusion anisotropy of human ubiquitin from 15N NMR relaxation. J Am Chem Soc 1995;117:12562–12566.
29. Barbato G, Ikura M, Kay LE, Pastor RW, Bax A. Backbone dynamics of calmodulin studied by 15N relaxation using inverse detected two-dimensional NMR spectroscopy: the central helix is flexible. Biochemistry 1992;31:5269–5278.
30. Zhou H, McEvoy MM, Lowry DF, Swanson RV, Simon MI, Dahlquist FW. Phosphotransfer and CheY-binding domains of the histidine autokinase CheA are joined by a flexible linker. Biochemistry 1996;35:433–443.
31. Farrow NA, Muhandiram R, Singer AU, Pascal SM, Kay CM, Gish G, Shoelson SE, Pawson T, Forman-Kay JD, Kay LE. Backbone dynamics of a free and phosphopeptide-complexed Src homology 2 domain studied by 15N NMR relaxation. Biochemistry 1994;33:5984–6003.
32. Lee LK, Rance M, Chazin WJ, Palmer AG. Rotational diffusion anisotropy of proteins from simultaneous analysis of 15N and 13C alpha nuclear spin relaxation. J Biomol NMR 1997;9:287–298.
33. (a) Nanduri S, Carpick B, Yang Y, Williams BRG, Qin J. 1H, 13C, 15N resonance assignment of the 20 kDa double stranded RNA binding domain of PKR. J Biomol NMR 1998;12:349–351; (b) Nanduri S, Carpick BW, Yang Y, Williams BRG, Qin J. Structure of the double-stranded RNA-binding domain of the protein kinase PKR reveals the molecular basis of its dsRNA-mediated activation. EMBO J 1998;17:5458–5465.
34. Kay LE, Keifer EP, Saarinen T. Pure absorption gradient enhanced heteronuclear single quantum correlation spectroscopy with improved sensitivity. J. Am Chem Soc 1992;114:10663–10665.
35. John BK, Plant D, Hurd RE. Improved proton-detected heteronuclear correlation using gradient-enhanced *z* and *zz* filters. J Mag Res A 1993;101:113–117.
36. Fischer MWF, Majumdar A, Zuiderweg ERP, Protein NMR relaxation; theory, application and outlook. Prog NMR Spect 1998;33:207–272.
37. Koradi R, Billerter M, Wuthrich K. MOLMOL: a program for display and analysis of macromolecular structures. J Mol Graph 1996;14:51–55.